J Surfact Deterg
DOI 10.1007/s11743-013-1439-3

ORIGINAL ARTICLE

Inhibition of Cast Iron Corrosion in Acid, Base, and Neutral Media Using Schiff Base Derivatives

Velayutham Rajeswari · Devarayan Kesavan · Mayakrishnan Gopiraman · Periasamy Viswanathamurthi

Received: 3 September 2012 / Accepted: 2 January 2013

Abstract Three Schiff bases, 2-acetylpyridine thiosemicarbazone (**I$_1$**), 2-acetylpyridine-(4-methylthiosemicarbazone) (**I$_2$**), and 2-acetylpyridine-(4-phenylthiosemicarbazone) (**I$_3$**) were tested against corrosion of cast iron in aqueous solutions of HCl, NaOH, NH_4Cl, and NaCl by means of a mass loss method and electrochemical measurements. The inhibition efficiency is directly proportional to inhibitor concentration, while it decreases with prolonged immersion time and at low temperatures. In order to study the effect of an additive, synergism of KI was also studied. The adsorption of Schiff bases in corrosive media obeys Langmuir's isotherm, both in the presence and absence of KI. The UV–Vis, FT-IR, WAXD and SEM analyses were carried out to support the mechanism of corrosion inhibition. The ΔG_{ads} values reveal that the inhibition was mainly due to physisorption of the inhibitor molecules on the surface of cast iron. The electrochemical polarization results showed the predominantly cathodic nature of the inhibitors.

Keywords Schiff bases · Corrosion · Adsorption · Cast iron · Synergism

Introduction

Corrosion of metals is one of the major problems due to the use of aggressive media in industrial processes. The corrosion of iron and its alloys is a fundamental academic topic and an industrial concern that has projected a lot of attention. Hence, inhibiting the steel corrosion has been an intensive field of interest [1]. It is well acknowledged that the corrosion of a metal can be significantly reduced once a small quantity of particular additives, named inhibitors are added to the chemical system [2].

Organic compounds, for example, Schiff bases and thiosemicarbazones are accounted as being valuable corrosion inhibitors for various metals [3–12] in acid media. The preference for a Schiff base inhibitor is ease of synthesis from relatively cheap materials. The action of such inhibitors depends on the interaction of functional groups with the metal surface. The interaction of inhibitors by the metal surface takes place through heteroatoms such as phosphorus, sulphur, nitrogen and oxygen as well as through triple bonds or aromatic rings.

The evaluation of inhibitors under various circumstances results in a wide range of opportunities for their utilization. Therefore, the authors have investigated the inhibitive nature of three Schiff base-thiosemicarbazone derivatives against the corrosion of cast iron in acid (HCl), base (NaOH) and neutral (NaCl and NH_4Cl) media. The inhibition mechanisms were studied by means of UV–Vis, FT-IR, wide angle X-ray diffraction (WAXD) and scanning electron microscopy (SEM) and the results are discussed in this article.

Experimental Techniques

Materials

All chemicals HCl (Merck), NaOH (Merck), NaCl (Spectrum), NH_4Cl (Spectrum)) were of analytical reagent grade

---

Electronic supplementary material The online version of this article (doi:10.1007/s11743-013-1439-3) contains supplementary material, which is available to authorized users.

V. Rajeswari · P. Viswanathamurthi (✉)
Department of Chemistry, Periyar University,
636011 Salem, India
e-mail: viswanathamurthi@rediffmail.com

D. Kesavan · M. Gopiraman
Department of Chemistry, National Institute of Technology,
620015 Tiruchirappalli, India

and used as received unless otherwise mentioned. The solutions of 1 N HCl, 0.005 N NaOH, 0.1 N NH_4Cl and 0.1 N NaCl were prepared using double distilled water.

Synthesis of Inhibitors

The Schiff base-thiosemicarbazone inhibitors (Fig. 1) were prepared according to an earlier report [13]. For example the Schiff base inhibitor, 2-acetylpyridine thiosemicarbazone was prepared by condensation of an equimolar solution of 2-acetylpyridine (0.22 mL) in ethanol (20 mL) and thiosemicarbazide (0.33 g) under reflux for 5 h to yield 2-acetylpyridine thiosemicarbazone (**I_1**). Similarly, 2-acetylpyridine-(4-methylthiosemicarbazone) (**I_2**) and 2-acetylpyridine-(4-phenylthiosemicarbazone) (**I_3**) were prepared from their corresponding thiosemicarbazides.

I_1: Yellow solid; Elemental analysis (MW 194.26 g mol^{-1} & MF $C_8H_{10}N_4S$), Calc. (Found): C, 49.96 (48.58), H, 5.18 (5.13), N, 28.84 (28.55), S, 16.37 (15.89). FT-IR (KBr): 3,248 cm^{-1} ($\nu_{N\text{–}H}$), 1,578 cm^{-1} ($\nu_{C=N}$), 833 cm^{-1} ($\nu_{C=S}$).

I_2: Yellow solid: Elemental analysis (MW 208.28 g mol^{-1} & MF $C_9H_{12}N_4S$), Calc. (Found): C, 51.91 (51.78), H, 5.80 (5.40), N, 26.91 (25.89), S, 15.39 (15.87). FT-IR (KBr): 3,201 cm^{-1} ($\nu_{N\text{–}H}$), 1,585 cm^{-1} ($\nu_{C=N}$), 833 cm^{-1} ($\nu_{C=S}$).

I_3: Yellow solid; Elemental analysis (MW 270.36 g mol^{-1} & MF $C_{14}H_{14}N_4S$), Calc. (Found): C, 62.21 (59.99), H 5.22 (5.20), N, 20.72 (20.52), S, 11.90 (11.87). FT-IR (KBr): 3,241 cm^{-1} ($\nu_{N\text{–}H}$), 1,580 cm^{-1} ($\nu_{C=N}$), 801 cm^{-1} ($\nu_{C=S}$).

Mass Loss Measurements

Cast iron specimens containing 6.09 % C, 1.13 % Al, 0.78 % Mn, with the remainder being Fe, were used for mass loss measurements, which were performed according to previous reports of one of the authors [8, 14–16]. In brief, rectangular cast iron coupons 2 × 1.5 × 0.02 cm in size were abraded using 600, 800, 1,000, and 1,200 grit emery papers, and then washed thoroughly with double distilled water, degreased with acetone and dried at room temperature and then weighed.

The experiment was performed at room temperature using different concentrations of inhibitors. The optimum time to achieve maximum inhibition efficiency was determined as 2 h. The cast iron specimen in triplicate was immersed in 100 mL of corrosion medium. The weights of the specimens were noted before and after the mass loss measurements. The experiments were repeated three times and the average values were considered for calculations. The percentage inhibition efficiency IE % was calculated using the following equation:

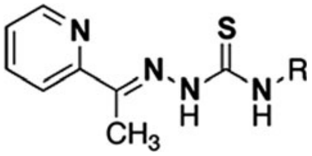

Fig. 1 Structure of Schiff base inhibitors. Where $R = \text{–H}$ (**I_1**), –CH_3 (**I_2**), $\text{–C}_6\text{H}_5$ (**I_3**)

$$\text{IE}\,\% = \frac{(M_0 - M)}{(M_0)} \times 100 \quad (1)$$

where, M_0 and M are the mass losses of cast iron in the absence and presence of inhibitors, respectively. In order to study the effect of additives, along with the inhibitor, small amount of KI solution was added to the experiment.

Electrochemical Measurements

Electrochemical experiment was carried out using a CH electrochemical analyzer model 760C. The cell consists of three electrodes: Cast iron specimen of an exposed area 1 × 1 cm^2 was used as the working electrode, platinum and saturated calomel electrodes were used as auxiliary and reference electrodes, respectively. The working electrode was abraded with a series of emery papers (600, 800, 1,000, and 1,200), and then degreased with double distilled water followed by acetone, prior to further use. All electrochemical measurements were conducted at 298 ± 1 K. The working electrode was first immersed into the test solution (corrosive media, both in presence and absence of inhibitor) to set a steady state open circuit potential for 45 min.

Potentiodynamic current–potential (Tafel) curves were recorded at a scan rate of 0.01 V s^{-1} and potential range was −0.2 to −0.8 V. The percentage inhibition efficiency IE % was calculated using Eq. (2)

$$\text{IE}\,\% = \frac{(I'_{\text{corr}} - I_{\text{corr}})}{(I'_{\text{corr}})} \times 100 \quad (2)$$

where I'_{corr} and I_{corr} are the current density values in the absence and presence of inhibitors, respectively.

The EIS experiments were conducted at an open circuit potential in the frequency range of 10^4–10^1 Hz and the amplitude was 0.005 V. Nyquist plots were made from these experiments. Double layer capacitance and inhibition efficiency were calculated using the following equations.

$$C_{\text{dl}} = \frac{1}{2\Pi f_{\max} R_{\text{ct}}} \quad (3)$$

$$\text{IE}\,\% = \frac{(R'_{\text{ct}} - R_{\text{ct}})}{R'_{\text{ct}}} \times 100 \quad (4)$$

where $f_{\max}$ is the frequency at apex on the Nyquist plot, R'_{ct} and R_{ct} are charge transfer resistance values of inhibited and uninhibited solutions, respectively.

Spectroscopies

In order to prepare the inhibitors adsorbed on the cast iron surface (Inh_{ads}), the cast iron coupons were immersed in a solution containing 120 ppm of an inhibitor in 1 N HCl. After 2 h of immersion, the specimens were removed, washed with distilled water followed by acetone and then air-dried. The adsorbed inhibitor (Inh_{ads}) was scraped carefully using a knife [8, 14–16]. Then the scraped sample was subjected to UV–Vis spectroscopy (PG instrument model T90 + spectrophotometer) as well as FT-IR spectroscopy (Perkin Elmer).

Wide Angle X-ray Diffraction (WAXD)

The inhibitors and the Inh_{ads} were subjected to WAXD analysis using a Rotaflex RTP300 X-ray diffractometer (Rigaku Co., Japan). X-ray diffractometer was controlled at 50 kV and 200 mA. Nickel filtered Cu Kα radiation was used for the measurements with an angular range of $5° < 2\theta < 70°$ at room temperature.

Surface Analysis

The morphologies of raw cast iron and specimens used for the mass loss measurements were observed under a Hitachi model-3000H scanning electron microscopy.

Results and Discussion

Mass Loss Measurements

Effect of Inhibitor Concentration

The inhibitors $\mathbf{I_1}$, $\mathbf{I_2}$ and $\mathbf{I_3}$ were tested against corrosion of cast iron in 1 N HCl, 0.005 N NaOH, 0.1 N NH_4Cl, and 0.1 N NaCl. The effect of concentration of inhibitors was studied for all the corrosive media, while for 1 N HCl the effect of temperature, and immersion time were also studied. The results are shown in Table 1. The Schiff base inhibitors ($\mathbf{I_1}$, $\mathbf{I_2}$ and $\mathbf{I_3}$) showed an increase in the IE % upon increasing the inhibitor concentration irrespective of the corrosion medium. This is attributed to the increased surface coverage by the inhibitor molecules. Inhibition efficiency values of the investigated inhibitors follows the order in all corrosion media: $\mathbf{I_3} > \mathbf{I_2} > \mathbf{I_1}$. Though the inhibitors show IE % over 50 against all the corrosive media (Fig. 2), the Schiff bases are best against acidic medium, followed by 0.1 N NH_4Cl, 0.005 N NaOH and 0.1 N NaCl (Table 2).

Effect of Temperature

To study the effect of temperature on the IE % in 1 N HCl, mass loss measurements were also carried out at temperatures 298–348 ± 1 K both in absence and presence of inhibitors (120 ppm). The IE % decreases on temperature

Table 1 Effect of inhibitor concentration on acid corrosion of cast iron at 298 ± 1 K

Name of inhibitors	Concentration of inhibitor (ppm)	Mass loss (g)	Surface coverage (θ)	IE %	Corrosion rate C_R (mm/y)
1 N HCl		0.0317			23.9
$\mathbf{I_1}$	20	0.0093	0.703	70.6	7.08
	40	0.0082	0.741	74.1	6.18
	60	0.0048	0.848	84.8	3.61
	80	0.0045	0.858	85.8	3.39
	100	0.0034	0.892	89.2	2.56
	120	0.0031	0.902	90.2	2.33
$\mathbf{I_2}$	20	0.0088	0.722	72.2	6.63
	40	0.0066	0.798	79.8	4.82
	60	0.0047	0.851	85.1	3.54
	80	0.0042	0.867	86.7	3.16
	100	0.0035	0.89	89.0	2.63
	120	0.0023	0.927	92.7	1.73
$\mathbf{I_3}$	20	0.0052	0.835	83.5	3.92
	40	0.0024	0.924	92.4	1.8
	60	0.0023	0.927	92.7	1.73
	80	0.002	0.936	93.6	1.5
	100	0.0016	0.95	95.0	1.2
	120	0.0016	0.95	95.0	1.2

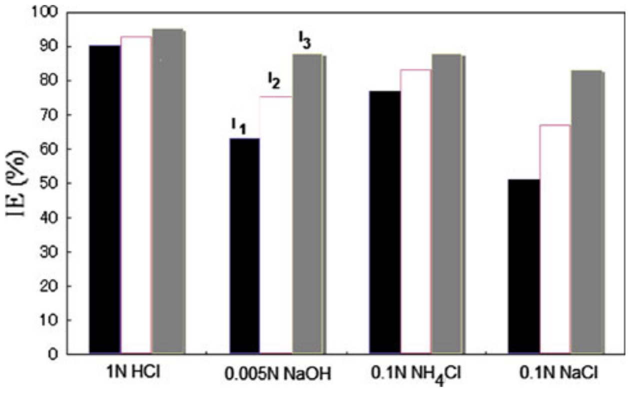

Fig. 2 Comparison of efficiencies of inhibitors for different media at 298 ± 1 K. (Inhibitors concentration-120 ppm for 1 N HCl, 10 ppm for 0.005 N NaOH, 0.1 N NH_4Cl, and 5 ppm for 0.1 N NaCl)

scale till 328 ± 1 K. This is due to the physical adsorption (weak van der Wall's forces) of inhibitor molecules on the surface of the cast iron. IE % gradually rises after 328 ± 1 K. This is attributed to the chemisorption of inhibitor molecules at elevated temperatures. The elements like N and S are proposed as being responsible for the chemical adsorption of the inhibitors on the metal surface. The results showed that the inhibitors adopt either physisorption or chemisorption or both depending on temperature of the corrosion system.

Effect of Immersion Time

The effect of time on the IE % was studied for acid corrosion inhibition of cast iron. The IE % values decreased (IE % for $\mathbf{I_1} = 69.4$, $\mathbf{I_2} = 78$, and $\mathbf{I_3} = 87$) for 4 h of immersion time, where as it showed an increase for 6 h of immersion time ($\mathbf{I_1} = 74.9$ %, $\mathbf{I_2} = 84.8$ %, and $\mathbf{I_3} = 90.3$ %). This is attributed to an adsorption–desorption phenomenon between the inhibitor molecules and the metal surface. Therefore, the specimens were subjected to mass loss measurements at prolonged immersion times (up to 16 h), to observe the trend of inhibition. The IE % values continued to decrease and no increase of IE % was observed.

Table 2 Effect of inhibitor concentration on NaOH, NH_4Cl, and NaCl corrosion of cast iron at 298 ± 1 K

Corrosion medium and inhibitors	Concentration (ppm)	Mass loss (g)	Surface coverage (θ)	IE %	Corrosion rate C_R (mm/y)
0.005 N NaOH		0.0008			6.033×10^{-4}
I_1	1	0.0007	0.13	13.0	5.27×10^{-4}
	5	0.0004	0.51	51.0	3.016×10^{-4}
	10	0.0003	0.63	63.0	2.226×10^{-4}
I_2	1	0.0005	0.38	38.0	3.77×10^{-4}
	5	0.0003	0.63	63.0	2.26×10^{-4}
	10	0.0002	0.75	75.0	1.058×10^{-4}
I_3	1	0.0004	0.52	52.0	3.016×10^{-4}
	5	0.0002	0.75	75.0	1.508×10^{-4}
	10	0.0001	0.88	88.0	0.754×10^{-4}
0.1 N NH_4Cl		0.0018			13.574×10^{-4}
I_1	1	0.001	0.44	44.0	0.7541×10^{-4}
	5	0.0007	0.61	61.0	5.2788×10^{-4}
	10	0.0004	0.77	77.0	3.0165×10^{-4}
I_2	1	0.0009	0.50	50.0	6.7871×10^{-4}
	5	0.0006	0.66	66.0	4.5247×10^{-4}
	10	0.0003	0.83	83.0	2.2623×10^{-4}
I_3	1	0.0007	0.63	63.0	5.2788×10^{-4}
	5	0.0004	0.78	78.0	3.0165×10^{-4}
	10	0.0002	0.88	88.0	1.5082×10^{-4}
0.1 N NaCl		0.0006			4.5247×10^{-4}
I_1	1	0.0004	0.33	33.0	3.0165×10^{-4}
	5	0.0003	0.5	50.0	2.2623×10^{-4}
I_2	1	0.0003	0.52	52.0	2.262×10^{-4}
	5	0.0002	0.67	67.0	1.5082×10^{-4}
I_3	1	0.0002	0.69	69.0	1.5082×10^{-4}
	5	0.0001	0.83	83.0	0.754×10^{-4}

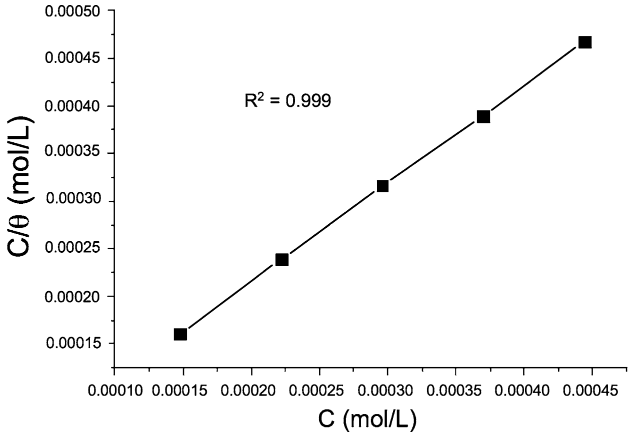

Fig. 3 Langmuir adsorption isotherms for mass loss measurement of $\mathbf{I_3}$

Adsorption Isotherm and Thermodynamic Parameters

The adsorption isotherms are very important in determining the corrosion inhibition mechanism, since it expresses the molecular interaction of the inhibitor molecule with the active sites on the cast iron surface. The degree of surface coverage (θ) was calculated from the mass loss measurements. Data were tested graphically by fitting to various isotherms including Frumkin, Langmuir, Temkin and Freundlich adsorption isotherms. The expected linear relationship was well fitted by a Langmuir isotherm (correlation coefficient R^2 equal to 0.998, 0.998, and 0.999 for $\mathbf{I_1}$, $\mathbf{I_2}$, and $\mathbf{I_3}$ respectively) through surface coverage of adsorbed inhibitor on cast iron surface. Accordingly, there should be no interaction between the molecules that were adsorbed at the metal surface. But the deviation of the slope values from unity indicated the presence of small interaction between the adsorbed molecules. The higher inhibitive property of the inhibitors is attributed to the presence of π electrons in aromatic ring, heteroatoms such as oxygen, sulphur and nitrogen and the larger molecular size, which covers larger surface of the metallic surface. Figure 3 shows a representative Langmuir isotherm of $\mathbf{I_3}$ drawn from the following equation.

$$\frac{C_{\mathrm{inh}}}{\theta} = \frac{1}{K} + C_{\mathrm{inh}} \qquad (5)$$

where, K is the adsorption constant and the slope of the line is respectively as follows for $\mathbf{I_1} = 1.028$, $\mathbf{I_2} = 1.024$, and $\mathbf{I_3} = 1.026$ at 298 ± 1 K. The slope values are mostly equal to unity, which means that an inhibitor molecule is adsorbed on an active site on the cast iron surface.

The activation energy (E_a), standard entropy of adsorption (ΔS_{ads}), standard free energy of adsorption (ΔG_{ads}), and standard heat of adsorption (Q_{ads}) were calculated by following Eqs. (6), (7), (8) and (9) according to previous reports [8, 14–16] and given in Table 3. Figure 4 shows the plot of ΔG_{ads} of inhibitors against different temperatures in 1 N HCl. The negative values of ΔG_{ads} indicate the spontaneity of adsorption of the inhibitor molecules on the cast iron surface [17, 18]. Typically, ΔG_{ads} values below -20 kJ mol^{-1} are due to the physisorption of the inhibitor, whereas ΔG_{ads} values above -40 kJ mol^{-1} are attributed to the chemisorption of the inhibitor molecules on metal surface. In the present case, ΔG_{ads} values are between 18 and 23 kJ mol^{-1}, which means that the inhibition mechanism at 298 ± 1 K proceeds via physical adsorption. This fact is also supported by effect of time as well as by temperature as discussed above. The higher E_a values of $\mathbf{I_2}$ and $\mathbf{I_3}$ indicates their better inhibition characteristics than $\mathbf{I_1}$. The negative Q_{ads} values indicate that the adsorption process is exothermic in nature. Large and negative values of ΔS_{ads} imply that the activated complex in the rate determining step represents an association rather than a dissociation step, meaning that

Table 3 Thermodynamic parameters for the cast iron in 1 N HCl in the presence of the inhibitors ($\mathbf{I_1}$–$\mathbf{I_3}$) at 298 ± 1 K

Inhibitor	Corrosion media	ΔG_{ads} (kJ mol^{-1})	$-E_a$ (kJ mol^{-1})	$-Q_{\mathrm{ads}}$ (kJ mol^{-1})	ΔH_{ads} (kJ mol^{-1})	$-\Delta S_{\mathrm{ads}}$ (kJ mol^{-1})
$\mathbf{I_1}$		−18.3	88.4	35.1	−21.62	72.5
$\mathbf{I_2}$	HCl	−18.9	19.1	28.2	−58.87	197.5
$\mathbf{I_3}$		−22.3	19.5	29.0	−58.90	197.6
$\mathbf{I_1}$		15.85				
$\mathbf{I_2}$	NaOH	19.12	–	–	–	–
$\mathbf{I_3}$		20.84				
$\mathbf{I_1}$		19.12				
$\mathbf{I_2}$	NH_4Cl	19.84	–	–	–	–
$\mathbf{I_3}$		22.56				
$\mathbf{I_1}$		18.57				
$\mathbf{I_2}$	NaCl	18.57	–	–	–	–
$\mathbf{I_3}$		18.57				

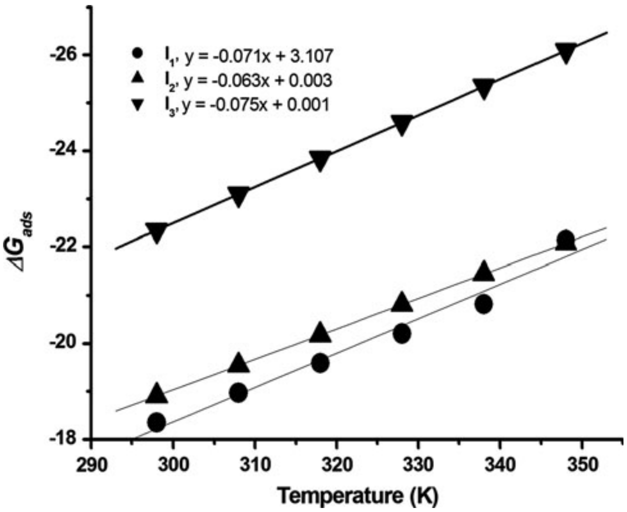

Fig. 4 Plot of ΔG_{ads} against different temperatures

a decrease in disordering takes place on going from reactants to the activated complex [19].

$$E_a = \Delta H_{\mathrm{ads}} + \mathrm{RT} \quad (6)$$

where E_a is activation energy, ΔH_{ads} is the standard enthalpy of adsorption, R is the gas constant (8.314 $\mathrm{JK^{-1}\ mol^{-1}}$), T is absolute temperature.

$$\mathrm{Intercept} = \log(\mathrm{R/Nh}) + (\Delta S_{\mathrm{ads}}/2.303\mathrm{R}) \quad (7)$$

$$\Delta G_{\mathrm{ads}} = -RT\,ln\,(55.5\,K) \quad (8)$$

where, 55.5 is the concentration of water in solution.

$$Q_{\mathrm{ads}} = 2.303\mathrm{R}\left[\log\left(\frac{\theta_2}{1-\theta_2}\right) - \log\left(\frac{\theta_1}{1-\theta_1}\right)\right]\frac{T_1T_2}{T_2-T_1} \quad (9)$$

where, θ_1, θ_2 are surface coverage of the inhibitor at 348, 298 K respectively, $\mathrm{T_1}$ is maximum temperature (348 K), $\mathrm{T_2}$ is minimum temperature (298 K).

Synergistic Effects of KI

It was reported that addition of halides to the corrosion system along with inhibitors, greatly diminishes the corrosion of metal [20, 21]. Therefore, in the present study, the synergistic effect of KI was studied against corrosion of cast iron in 1 N HCl, 0.005 N NaOH, 0.1 N NH_4Cl and 0.1 N NaCl. The results are shown in Fig. S1. and Table 4. The addition of KI has improved the IE % values for all the corrosion media except for NaOH corrosion system. Especially, for neutral media (NH_4Cl and NaCl), addition of KI was much more effective than for acid medium. In the case of 0.005 N NaOH corrosion medium, no significant changes in IE % were observed in presence of KI even at higher concentrations of KI. Similarly, for 1 N HCl, 0.1 N NH_4Cl and 0.1 N NaCl beyond certain KI concentration, there is no observable changes in mass loss measurements. Synergistic factor (given in Table 4) was calculated by the following equation.

$$\text{Synergistic factor} = \frac{(1 - I_{1+2})}{(1 - I'_{1+2})} \quad (10)$$

where $\mathrm{I_1}$ = Inhibition efficiency (IE %) of KI alone, $\mathrm{I_2}$ = Inhibition efficiency (IE %) of inhibitor alone, $\mathrm{I'_{1+2}}$ = IE % of inhibitor + KI.

Potentiodynamic Polarization Studies

Anodic and cathodic polarization curves for cast iron in 1 N HCl were obtained both in presence and absence of

Table 4 Comparison of effect of KI on corrosion inhibition of cast iron in presence of optimum concentration of inhibitors at 298 ± 1 K

Corrosion medium	Concentration of KI (ppm)	Synergistic parameter (S_1)			IE %		
		I_1	I_2	I_3	I_1	I_2	I_3
	5				84.0	92	92
	10				89.0	94	95
1 N HCl	15	1.11	1.12	1.13	91.0	94	96
	20				93.0	95	97
	25				94.0	96	98
	30				95.0	97	98
	1				13.0	38	52
0.005NNaOH	5	1.08	1.06	1.05	51.0	63	75
	10				63.0	75	88
0.1 N NH_4Cl	1	0.97	1.02	1.09	83.0	88	94
	2				93.0	94	97
	1				17.0	33	50
0.1 N NaCl	2	1.03	1.06	0.99	35.0	51	83
	3				53.0	85	89

inhibitors $\mathbf{I_1}$, $\mathbf{I_2}$, or $\mathbf{I_3}$. The Tafel plots are shown in Fig. 5. The various electrochemical parameters such as corrosion potential (E_{corr}), corrosion current density (I_{corr}), cathodic, anodic Tafel slopes (b_c and b_a) and corresponding IE % were determined from the polarization results and are listed in Table 5. Upon increasing the concentration of Schiff base inhibitors, both cathodic and anodic reactions were affected as shown in the Tafel plots. This result implies that the addition of the inhibitors diminish anodic dissolution of iron as well as the cathodic hydrogen evolution reaction [22]. The high IE % of $\mathbf{I_3}$ may be due to the existence of a phenyl ring having high electron density [23, 24]. The shift of the E_{corr} values is not more than 85 mV, therefore, the studied Schiff bases are classified as mixed-type inhibitors.

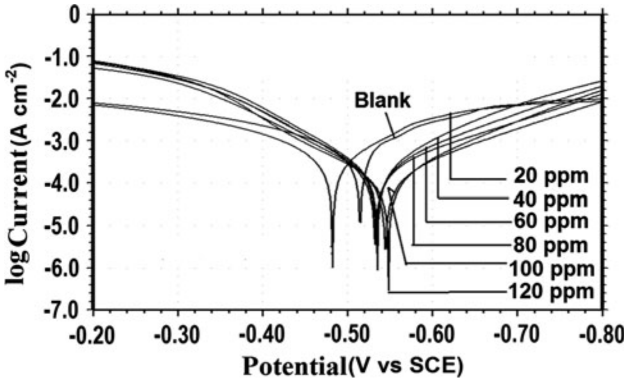

Fig. 5 Tafel polarization curves for cast iron in 1 N HCl in the presence and absence of inhibitor $\mathbf{I_3}$

Electrochemical Impedance Spectroscopy (EIS)

Nyquist plots of cast iron in uninhibited and inhibited acidic solutions containing various concentrations of Schiff base inhibitor are shown in Fig. 6a. Results obtained from EIS can be interpreted in terms of the equivalent circuit is shown in Fig. 6b. In the given electrical circuit, R_s is the solution resistance, R_{ct} is the charge transfer resistance, and C_{dl} is the double layer capacitance. It is obvious from these plots that the impedance response of cast iron in uninhibited 1 N HCl has considerably changed after the addition of inhibitors into the corrosive solutions. Nyquist plots size increase with the inhibitor concentration, suggested that the produced inhibitive film was strengthened by addition of inhibitors and also charge transfer process mainly controlling the corrosion of cast iron. The charge-transfer resistance (R_{ct}) values were calculated from the difference in impedance at lower and higher frequencies [25]. Inspection of the Table 6, the R_{ct} values increased and the values of C_{dl} decreased with an increase in the inhibitor's concentration. This condition was a result of increasing surface coverage by the inhibitor, which led to an increase in IE %. The impedance study also provided more or less same efficiency as found in both potentiodynamic polarization and weight loss measurements. Electrochemical impedance spectroscopy and polarization curves measurements were repeated a number of times and observed that

Table 5 Tafel polarization parameter values for the corrosion of cast iron in the absence and presence of inhibitors in 1 N HCl at 298 ± 1 K

Inhibitor	Concentration (ppm)	$-E_{\mathrm{corr}}$ (mV vs. SCE)	b_c (mV/decade)	b_a (mV/decade)	I_{corr} (μA/cm^2)	IE %
Blank	–	515	5.252	5.514	509	–
$\mathbf{I_1}$	20	496	5.713	5.729	149.1	70.7
	40	502	5.864	5.676	130.0	74.4
	60	495	7.679	5.066	81.4	85.1
	80	500	5.759	5.032	72.1	85.8
	100	509	5.083	5.201	52.4	89.7
	120	595	4.408	3.774	50.2	90.1
$\mathbf{I_2}$	20	471	4.711	5.755	133.7	73.7
	40	473	6.257	5.660	102.3	79.9
	60	516	7.669	5.437	75.8	85.1
	80	493	7.092	4.915	67.8	86.6
	100	511	5.367	5.267	51.0	89.9
	120	515	7.189	12.047	29.7	94.0
$\mathbf{I_3}$	20	482	8.694	5.856	84.6	83.3
	40	535	9.269	11.369	40.8	91.9
	60	534	7.950	10.919	39.8	92.1
	80	532	7.012	11.494	36.3	92.8
	100	544	7.719	10.498	24.7	95.1
	120	548	8.951	10.198	23.2	95.4

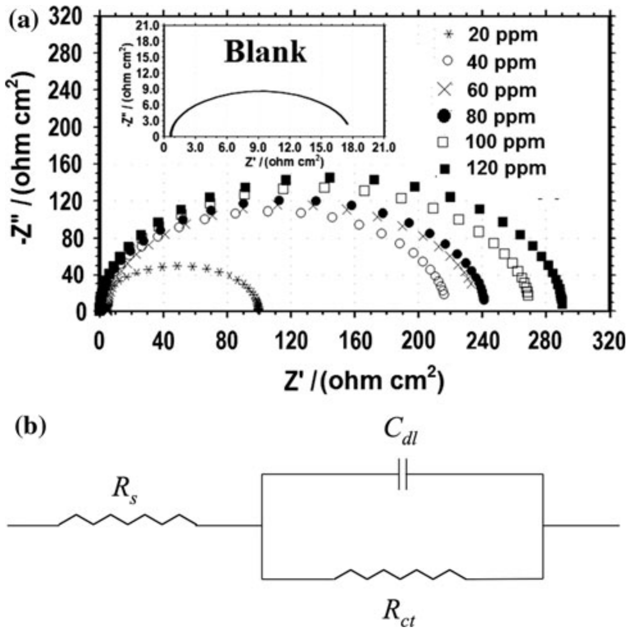

Fig. 6 EIS measurements. **a** Nyquist plots of cast iron in 1 N HCl in the presence and absence of inhibitor $\mathbf{I_3}$ and **b** the equivalent circuit model used for EIS measurements

they were greatly reproducible. Therefore it is essential to point out that the three compounds under study revealed the identical behavior in all test times and for all concentrations.

Table 6 EIS parameters for cast iron at different concentration of Schiff base inhibitors in 1 N HCl at 298 ± 1 K

Inhibitor	Concentration (ppm)	R_{ct} (Ω cm^2)	f_{max}	C_{dl} (μF/cm^2)	IE %
Blank	–	16.88	8.57	1,099.60	–
$\mathbf{I_1}$	20	59.36	29.79	90.04	71.5
	40	65.33	33.39	72.89	74.1
	60	109.54	54.83	26.51	84.5
	80	117.04	58.56	23.23	85.5
	100	161.89	83.58	11.76	89.5
	120	169.93	87.61	10.69	90.0
$\mathbf{I_2}$	20	58.38	29.49	92.48	71.0
	40	81.42	42.02	46.54	79.2
	60	117.97	58.80	22.95	85.6
	80	123.77	63.71	20.19	86.3
	100	166.86	83.20	11.47	89.8
	120	237.16	118.6	5.60	92.8
$\mathbf{I_3}$	20	99.74	49.95	31.96	83.0
	40	215.80	108.8	6.78	92.1
	60	228.42	115.6	6.03	92.6
	80	241.34	120.7	5.46	93.0
	100	268.30	134.8	4.40	94.0
	120	290.54	145.2	3.77	94.2

UV–Visible Spectroscopy

UV–Vis spectroscopy is a suitable method for detecting the complex formation of inhibitors with Fe^{2+} ions in 1 N HCl after the corrosion process. Change in position of the absorption maximum and or change in the value of absorbance indicates the formation of a complex between two species in solution. Figure S2 shows the UV–Visible spectra of inhibitor and Inh_{ads}. Inhibitors show two main absorption bands around 240–260 and 300–380 nm, which can be assigned to $\pi \rightarrow \pi^*$ (phenyl) and $n \rightarrow \pi^*$ (C=N) transitions respectively. In the case of Inh_{ads} samples, the band around 300–380 nm ($n \rightarrow \pi^*$) had completely disappeared and there was also a small red shift in the band around 280–340 nm, indicating charge transfer from inhibitors to the cast iron surface mainly through N and S. This is attributed to the formation of coordination bonds between the Schiff base inhibitors and the steel surface [26].

FT-IR Spectroscopy

The FT-IR spectra were recorded for inhibitors and Inh_{ads} samples to study the type of interactions (chemical and physical) of Schiff base derivatives on mild steel surface in 1 N HCl. Figure S3 shows all the characteristic bands corresponding to the functional groups (C=S, C=N and N–H) present in the Schiff base and also peaks were noted for Inh_{ads} in 1 N HCl. The inhibitors showed a strong band in the region 1,570–1,580 cm^{-1} due to C=N [27]. This band has been shifted to lower wavelength around 1,580–1,620 cm^{-1} for the adsorbed inhibitor, which clearly confirms the formation of coordination bond between the cast iron and the inhibitor molecules. In addition, broadening of N–H stretching vibration also confirms the coordination type bond formation.

Wide Angle X-ray Diffraction (WAXD)

The X-ray diffractograms of the Schiff base derivatives and Inh_{ads} were scanned in the range $5° < 2\Theta < 70°$ at a wavelength of 1.543 Å. Figure 7 shows very high relative intensity peaks in the region 5–30° for Schiff base derivative indicating crystalline nature. But in the case of Inh_{ads}, broad peaks were observed in the region 5–30°, which reveals the formation of chemisorbed layer on cast iron surface [16, 28, 29]. Analysis of the inhibitors-adsorbed (Inh_{ads}) on the cast iron are useful in revealing the inhibition mechanism. The changes in the X-ray diffraction suggested that the inhibitors may chemically adsorb onto the surface of the cast iron. The amorphous nature of the scraped samples indicated that the inhibitors chemically interacted with the metal rather than a physical interaction.

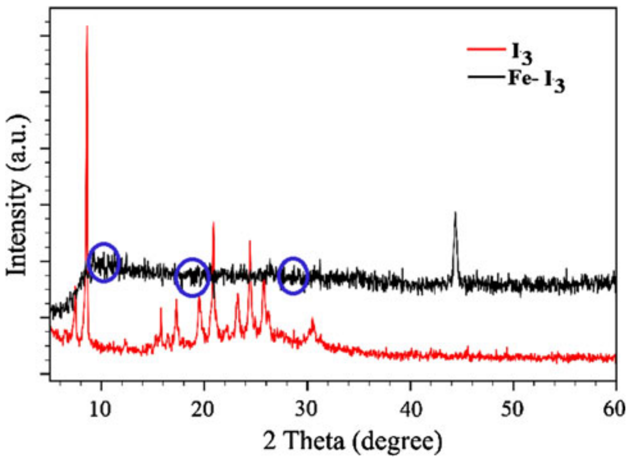

Fig. 7 WAXD of $\mathbf{I_3}$ & Fe-$\mathbf{I_3}$

Surface Analysis

In order to establish the interaction of inhibitor molecules with the metal surface during the corrosion inhibition process, both in the presence and absence of inhibitors SEM morphologies of the cast iron specimens were taken, and they showed that the cast iron sample immersed in 1 N HCl had been severely damaged due to the aggressive acid attack. The SEM pictures also show a comparatively smooth surface of the cast iron after adding of optimum concentration (120 ppm) of inhibitors to the 1 N HCl solution. It can be concluded from the SEM images that the inhibitor molecules slow down the dissolution of steel by forming organic layer on the iron surface. Therefore, the inhibitors protect the cast iron from acid solution.

Conclusion

$\mathbf{I_1}$, $\mathbf{I_2}$ and $\mathbf{I_3}$ perform as good corrosion inhibitors for cast iron in all media. The results confirm that a high inhibition efficiency was achieved at a concentration of 120 ppm. The inhibition efficiency follows the order: $\mathbf{I_3} > \mathbf{I_2} > \mathbf{I_1}$. Differences in the inhibition efficiency are correlated to the phenyl and methyl substituents present in inhibitors. Electrochemical polarization method revealed the mixed mode of inhibition of inhibitors. Adsorption of inhibitor molecules on the cast iron surface was found to obey the Langmuir adsorption isotherm. Thermodynamic parameter values of free energy of adsorption revealed that at 298 ± 1 K the inhibitor molecules adsorbed on cast iron surface via physisorption mechanism and at 338–348 K the inhibitor molecules adsorbed on iron surface via chemisorbed mechanism. Synergistic effects by KI were found to be effective in all the corrosive media except basic corrosion environment. UV–Visible, FT-IR spectroscopy and WAXD were evidences for chemisorption mechanism and temperature method was evidence for both physisorption as well as chemisorption mechanism. Additionally, SEM images provide information of protective layer formation on the cast iron surface. As a final point, these Schiff base inhibitors are effective against the corrosion of cast iron in corrosive media such as acidic (HCl), basic (NaOH), and neutral media (NH_4Cl and NaCl).

References

1. Uhlig HH, Revic RW (1985) Corrosion and corrosion control. Wiley, New York, p 115
2. Rozenfeld IL (1981) Corrosion inhibitors. McGraw-Hill, New York, p 182
3. Negm NA, Zaki MF (2008) Corrosion inhibition efficiency of nonionic Schiff base amphiphiles of p-aminobenzoic acid for aluminum in 4N HCl. Colloids Surf A 322:97–102
4. Negm NA, Zaki MF (2009) Synthesis and evaluation of 4-diethyl amino benzaldehyde Schiff base cationic amphiphiles as corrosion inhibitors for carbon steel in different acidic media. J Surfact Deterg 12:321–329
5. Negm NA, El-Farragry AF, Abdelrahman NR (2011) New Schiff base cationic surfactants: surface and thermodynamic properties and applicability in bacterial growth and metal corrosion prevention. J Surfact Deterg 14:505–514
6. Aiad IA, Negm NA (2009) Some Schiff base surfactants as steel-corrosion inhibitors. J Surfact Deterg 12:313–319
7. Hosseini MG, Ehteshamzadeh M, Shahrabi T (2007) Protection of mild steel corrosion with Schiff bases in 0.5 M H_2SO_4 solution. Electrochim Acta 52:3680–3685
8. Kesavan D, Muthu Tamizh M, Gopiraman M, Sulochana N, Karvembu R (2013) Physicochemical studies of 4-substituted N-(2-mercaptophenyl)-salicylideneimines: corrosion inhibition of mild steel in an acid medium. J Surfact Deterg (published on line) doi:10.1007/s11743-012-1338-z
9. Ekpe UJ, Ibok UJ, Ita BI, Offiong OE, Ebenso EE (1995) Inhibitory action of methyl and phenyl thiosemicarbazone derivatives on the corrosion of mild steel in hydrochloric acid. Mater Chem Phys 40:87–93
10. Ebenso EE, Ekpe UJ, Ita BI, Offiong OE, Ibok UJ (1999) Effect of molecular structure on the efficiency of amides and thiosemicarbazones used for corrosion inhibition of mild steel in hydrochloric acid. Mater Chem Phys 60:79–90
11. Khaled KF, El-maghraby A, Ibrahim OB, Elhabib OA, Ibrahim MAM (2010) Inhibitive effect of thiosemicarbazone derivative on corrosion of mild steel in hydrochloric acid solution. J Mater Environ Sci 1:139–150
12. Stanly JK, Geetha P (2010) Corrosion inhibition of mild steel in hydrochloric acid solution by Schiff base furoin thiosemicarbazone. Corros Sci 52:224–228
13. Kowol CR, Berger R, Eichinger R, Roller A, Jakupec MA, Schmidt PP, Arion VB, Keppler BK (2007) Gallium(III) and Iron(III) complexes of α-N-heterocyclic thiosemicarbazones: synthesis, characterization, cytotoxicity and interaction with ribonucleotide reductase. J Med Chem 50:1254–1265
14. Kesavan D, Muthu Tamizh M, Sulochana N, Karvembu R (2012) 2-[(*E*)-{(1*S*,2*R*)-1-hydroxy-1-phenylpropan-2-ylimino}methyl] phenol for inhibition of acid corrosion of mild steel. J Surfact Deterg. doi:10.1007/s11743-012-1370-z

15. Gopiraman M, Selvakumaran N, Kesavan D, Karvembu R (2012) Adsorption and corrosion inhibition behaviour of N-(phenylcarbamothioyl)benzamide on mild steel in acidic medium. Prog Org Coat 73:104–111
16. Gopiraman M, Selvakumaran N, Kesavan D, Kim IS, Karvembu R (2012) Chemical and physical interactions of 1-benzoyl-3,3-disubstituted thiourea derivatives on mild steel surface: corrosion inhibition in acidic media. Ind Eng Chem Res. doi:10.1021/ie300048t
17. Tang L, Li X, Mu G, Li L, Liu G (2006) Synergistic effect between 4-(2-pyridylazo) resorcin and chloride ion on the corrosion of cold rolled steel in 0.5 M sulfuric acid. Appl Surf Sci 252:6394–6401
18. Ali SA, Al-Muallem HA, Saeed MT, Rahman SU (2008) Hydrophobic-tailed bicycloisoxazolidines: a comparative study of the newly synthesized compounds on the inhibition of mild steel corrosion in hydrochloric and sulfuric acid media. Corros Sci 50:664–675
19. Martinez S, Stern I (2002) Thermodynamic characterization of metal dissolution and inhibitor adsorption processes in the low carbon steel/mimosa tannin/sulfuric acid system. Appl Surf Sci 199:83–89
20. Gomma GK (1998) Corrosion of low-carbon steel in sulphuric acid solution in presence of pyrazole-halides mixture. Mater Chem Phys 55:241–246
21. Hosseini M, Mertens SFL, Arshadi MR (2003) Synergism and antagonism in mild steel corrosion inhibition by sodiumdodecylbenzenesulphonate and hexamethylenetetramine. Corros Sci 45:1473–1489
22. Quraishi MA, Jamal D (2003) Dianils as new and effective corrosion inhibitors for mild steel in acidic solutions. Mater Chem Phys 78:608–613
23. Wu TX, Li ZJ, Zhao JC (1998) A facile method for the synthesis of 4-amino-5-hydrocarbon 2,4-dihydro-3H-1,2,4-triazole-3-thion Schiff bases. Chem J Chin Univ 19:1617–1625
24. Wang J, Cao C, Chen J, Zhang M, Ye G, Lin H (1995) Anodic desorption of inhibitors I. The phenomenon of anodic desorption of inhibitors. J Chin Soc Corros Prot 15:241–248
25. Emregul KC, Duzgun E, Atakol O (2006) The application of some polydentate Schiff base compounds containing aminic nitrogens as corrosion inhibitors for mild steel in acidic media. Corros Sci 48:3243–3260
26. Ashok Kumar SL, Gopiraman M, Saravana Kumar M, Sreekanth A (2011) 2-acetylpyridine-N(4)-morpholine thiosemicarbazone (HAcpMTSc) as a corrosion inhibitor on mild steel in HCl. Ind Eng Chem Res 50:7824–7832
27. West DX, Stark AM, Bain GA, Liberta AE (1996) Copper(II) complexes of 2-formyl-, 6-methyl-2-formyl- and 2-benzoylpyridine N(4)-(2-methylpyridinyl)-, N(4)-(2-methylpyridinyl)-, and N(4)-methyl(2-ethylpyridinyl)thiosemicarbazones. Transit Met Chem 21:289–295
28. Kim EJ, Herrera JE (2010) Characteristics of lead corrosion scales formed during drinking water distribution and their potential influence on the release of lead and other contaminants. Environ Sci Technol 44:6054–6061
29. Kim DK, Muralidharan S, Ha TH, Bae JH, Ha YC, Lee HG, Scantlebury JD (2006) Electrochemical studies on the alternating current corrosion of mild steel under cathodic protection condition in marine environments. Electrochim Acta 51:5259–5267

Author Biographies

Velayutham Rajeswari obtained an M.Sc. (2008) from Periyar University, Salem, India and completed a M.Phil., from Annamalai University, Chidambaram, India. She is pursuing a Ph.D. in Corrosion Science at Periyar University, Salem, India.

Devarayan Kesavan obtained an M.Sc. (2009) from the National Institute of Technology, Tiruchirappalli, India. He is pursuing a Ph.D. in biopolymers at Shinshu University, Japan.

Mayakrishnan Gopiraman obtained an M.Sc. (2010) from National Institute of Technology, Tiruchirappalli, India. He is working on a Ph.D. in heterogeneous nano-catalysis at Shinshu University, Japan.

Periasamy Viswanathamurthi earned a Ph.D. in inorganic chemistry (1999) from Bharathiar University, Coimbatore, India. He carried out his postdoctoral research at Chonbuk National University, South Korea, as well as at Shinshu University, Japan. He has also been a visiting professor at Sophia University, Japan. He is a professor of chemistry at Periyar University, Salem, India.